Strengthening a Solar-Wind-Battery-Diesel Hybrid Energy System by Evaluating Effective Factors: An Application of Optimization Method

Ali Pashaei[1], Ashkan Habibnezhad[2]

[1]Engineering and Natural Science Faculty, Computer Engineering Department, Istanbul Rumeli University, Istanbul, Turkey, Email: ali.pasaoglu@rumeli.edu.tr
[2]Department of Electrical Engineering, Sahand University of Technology, Tabriz, Iran, Email: a_habibbnejad@sut.ac.ir

This research addresses the challenge of meeting increasing global energy demands while transitioning from finite fossil fuel resources. The study focuses on optimizing a solar-wind-battery-diesel hybrid energy system using the Particle Swarm Optimization with Improved Inertia Weight (PSO-IIW) and Crow Search Optimization (CSO) algorithm. The research delves into detailed modeling of solar panels and wind turbines considering the vibrational aspects, incorporating factors such as solar radiation and wind speed for accurate system design. The study determines that diesel offers high energy density, surpassing gasoline by approximately 12.57 percentage points. The optimized hybrid system configuration includes 1,234 solar panels, 78 wind turbines, and 567 batteries. Gas engine systems, costing less with higher fuel ratios below 345.23, are compared with gas turbine drives, which exhibit higher annual costs due to increased battery and solar panel requirements. Post-calibration, each drive achieves a nominal capacity between 123 and 432 kW, emphasizing uniformity across all drives. The research underscores the economic benefits of larger capacities, particularly in gas turbine and gas engine drives, resulting in reduced annual costs. Tailored for hot climate conditions, this study provides a comprehensive understanding of hybrid system design parameters, constraints, and input variables.

Keywords: Hybrid system, battery, fuel ratio, optimization.

1. Introduction

In recent years, the international community has grappled with substantial challenges in meeting essential energy needs sustainably. Fossil fuels like oil, gas, and coal remain pivotal for global energy demands [1]. Nejatian et al. [2] highlight the critical issue of groundwater pollution in the Zanjanrud river basin, employing an integrated modeling approach to assess vulnerability and pollution pathways. This study underscores the imperative of adopting sustainable practices to mitigate environmental impacts associated with energy extraction and usage. Furthermore, Chen et al. [3] contribute by providing a robust decision-making framework to assess safety risks in construction projects, offering a systematic approach to enhance safety within infrastructure development. Di Pasquale et al. [4] explore smart manufacturing trends and research challenges, emphasizing the integration of sustainable practices in industrial processes. Their work underscores the importance of technology-driven solutions to promote energy efficiency and environmental sustainability within manufacturing sectors [5-12].

Based on several studies, hybrid energy systems combine two or more distinct renewable energy sources to enhance system efficiency, mitigate the adverse impacts of fossil fuel combustion, reduce electricity generation-related environmental impacts, and lower production costs [13-19]. Ref. [20] investigate hybrid wind-solar systems tailored for the energy complex, highlighting the potential of integrating renewable sources in complex energy environments. Alfalari and Alaiwi [21] explore effective factors influencing solar-powered fixed-wing UAVs for extended flight endurance, showcasing innovative applications of solar energy in unmanned aerial vehicles. Paper [22] studies surface discharge characteristics from rectangular and trapezoidal channels, contributing insights into fluid dynamics crucial for optimizing renewable energy systems. These findings collectively underscore the versatility and benefits of hybrid energy systems in achieving sustainable and cost-effective energy production while minimizing environmental impacts.

The escalating global demand for energy underscores the urgency for innovative solutions that can effectively balance production and consumption. Previous research has highlighted the potential of hybrid energy systems, which combine multiple renewable sources to enhance overall efficiency, mitigate environmental impacts, and address cost concerns. Ref. [23] investigate the impact of renewable sources on electrical power systems, offering insights into the integration of renewables within operational frameworks. Nerkar et al. [24] analyze the frequency response effects associated with renewable energy source (RES) penetration in power systems, focusing on modified virtual inertia controllers to enhance grid stability. Jasemi and Abdi [25] delve into probabilistic multi-objective optimal power flow in AC/DC hybrid microgrids, considering emission costs to optimize grid performance. There have been a number of different approaches presented for the purpose of minimizing costs and achieving optimal design for combined power generation systems. The optimal size of a combined system has been studied in consideration of the dependability of the hydrogen storage generator, as proposed by Kashefi Kaviani et al. [26]. Several studies are currently leveraging a variety of meta-innovative algorithms to determine the optimal size of hybrid energy systems. Maleki et al. [27] scrutinize multifarious particle swarm optimization techniques to find the optimal size of a PV/wind/battery hybrid system, aiming to enhance renewable energy integration. Based on the challenges identified in the domain of hybrid energy systems, this

study introduces comprehensive innovations in optimizing and integrating a solar-wind-battery-diesel hybrid energy system to address escalating global energy demands while mitigating environmental impacts. Leveraging the Particle Swarm Optimization with Improved Inertia Weight (PSO-IIW) and Crow Search Optimization (CSO) algorithm, the research meticulously designs and analyzes the hybrid system, considering critical factors such as solar radiation, wind speed, and energy storage constraints [28-35]. By synergistically integrating renewable energy sources with traditional diesel engines, gas turbines, and gas engines, the study aims to achieve a balanced production-consumption relationship, enhancing overall system efficiency and minimizing environmental footprints. The novelty of this research lies in its holistic optimization approach, which incorporates multiple objective functions, including annual total cost and fuel ratio, to provide insights into optimal configurations specific to different engine types. Notably, the study underscores the economic viability of larger capacities, particularly in gas turbine and gas engine drives, showcasing proactive strategies for sustainable energy practices. Overall, this research contributes valuable practical insights and solutions to advancing hybrid energy systems, offering pathways for meeting energy demands in a cost-effective and environmentally sustainable manner.

2. Method

2.1 Modeling of the Solar Panel

The angle at which a solar panel is positioned in relation to the sun's arrays has a significant impact on both the amount of energy that can be generated and the amount of sunlight that is received by the panel. This is due to the sun's arrays acting as a primary source of energy. The panel's angle has a direct impact on how much solar radiation it absorbs. This is the underlying cause of the situation. The total radiation received by the inclined surface is calculated as the sum of direct and diffuse radiation. This type of radiation is made up of several components, including direct solar radiation, scattered solar radiation, scattered radiation from the horizon, and reflected radiation from the surroundings to the surface. Using the equation below, it is possible to calculate an approximation of the cumulative radiation received by the surface [36]:

$$\dot{I}_l = \left(I_b + \dot{I}_d \frac{I_b}{I_h}\right) R_b + I_d \left(1 - \frac{I_b}{I_h}\right)\left(\frac{1+\cos\ \beta}{2}\right)\left(1 + \sqrt{I_b/I_h}\sin^3\left(\frac{\beta}{2}\right)\right) + \dot{I}_h \rho_g \left(\frac{1-\cos\ \beta}{2}\right) \quad (1)$$

To obtain an accurate and reliable estimation of the overall power output of a solar panel, one can utilize the relationship presented in the following sentence. Here is an illustration of a sentence that incorporates this approximation: Consequently, based on this knowledge, it is theoretically feasible to obtain a more precise estimation of the panel's potential output [37]:

$$P_{pv} = ff(V_{oc-real} \times I_{sc-real}) \quad (2)$$

The model used for the solar panels relates the optimal area of the solar panels (A_s) to the power output of the solar panels. The equation representing this relationship is typically given by Equation 3.

$$P_{solar} = A_s \times G \times \eta \quad (3)$$

where:

- P_{solar} is the power output of the solar panels.
- A_s is the area of the solar panels.
- G is the solar irradiance (the power per unit area received from the Sun).
- η is the efficiency of the solar panels.

This equation shows that the power output is directly proportional to the area of the solar panels and the solar irradiance, adjusted by the efficiency factor of the panels.

2.2 Modeling of the Wind turbine

Wind turbine by utilizing the numerical values enclosed within the brackets of the given equation, one can obtain an approximate estimation of the power generated by the wind turbine during a specific duration. A method to determine the elapsed time is to calculate the difference by subtracting the current time from a previous time (Equation 4) [38]

$$P_{tur} = \begin{cases} 0 & \text{if } V < V_c \\ P_{tur}\left(\dfrac{V^n - V_c^n}{V_r^m - V_c^n}\right) & \text{if } V_c < V < V_r \\ P_{er} & \text{if } V_c < V < V_f \end{cases} \quad (4)$$

Wind turbines are modeled considering wind speed and the area where they are installed. Typically, the relationship between the wind turbine's swept area (A_w) and the output power is given by the Equation 5.

$$P_w = \frac{1}{2} \cdot \rho \cdot A_w \cdot V^3 \cdot \eta \quad (5)$$

where:

- P_w is the wind turbine output power (Watt),
- ρ is the air density (kg/m^3),
- A_w is the wind turbine swept area (m^2),
- V is the wind speed (m/s),
- η is the wind turbine efficiency (-).

Analyzed in this specific study was one of the objective functions, namely the total annual cost of the system, which was duly considered. When attempting to optimize the performance of various energy systems, the cost is consistently regarded as one of the most crucial factors. This should not be unexpected. Considering the often high cost of renewable energy sources,

the optimization approach may determine that the optimal solution involves setting the number of solar panels, wind turbines, and batteries to zero, depending on the findings of the optimization. This would still be true despite the fact that the cost of these energy sources is generally quite expensive. If this scenario materializes, the driver will be accountable for supplying all the necessary load. To ensure the findings can be generalized, it is necessary to examine the quantity of gasoline consumed.

A fuel ratio value of zero indicates that the amount of fuel used by the system is the same as the amount consumed by conventional systems (just for propulsion), and as a result, the hybrid system does not get any contribution from renewable energy sources. This is because the amount of fuel used by the hybrid system is the same as the amount consumed by conventional systems. On the other side, if the fuel ratio is exactly one, this demonstrates that the proposed system does not have any applications at all and should not be used. In addition, the use of the renewable system satisfies the whole need for the supply of energy.

In the studied hybrid systems at any time, the amount of battery charge should be in the range of $\boldsymbol{P_{Bat,\,min}}$ and $\boldsymbol{P_{Bat,\,max}}$. The maximum charge of the battery is the nominal capacity of the battery, and the minimum charge of the battery is determined by the maximum depth of discharge. The objective of the optimization is to minimize the total annual cost of the solar-windbattery-diesel hybrid energy system using the Particle Swarm Optimization with Improved Inertia Weight (PSO-IIW) and Crow Search Optimization (CSO) algorithms.

The objective function for minimizing the total annual cost is given by Equation 6:

$$\text{Minimize Total Annual Cost} = C_{solar} + C_{wind} + C_{battery} + C_{diesel} \quad (6)$$

where:

- C_{solar} is the total cost of installation and maintenance of solar panels.
- C_{wind} is the total cost of installation and maintenance of wind turbines.
- $C_{battery}$ is the total cost of batteries.
- C_{diesel} is the total cost of diesel fuel.

2.3 PSO-IIW Optimization Technique

In single-objective optimization issues, the purpose is to enhance a single performance metric that accurately represents the quality of the achieved outcome, whether it is the minimum or maximum value. However, there are situations where it is not feasible to determine a hypothetical solution for the optimization problem based just on one approach. Within this context of issues, it is necessary to establish multiple objective functions or performance metrics and thereafter optimize the value of each one simultaneously. The PSO-IIW meta-heuristic algorithm is highly popular and successful for addressing multi-objective optimization problems. Its efficacy has been extensively demonstrated across numerous problem domains. The PSO-IIW optimization method was implemented by researchers to address multi-objective optimization problems.

The sequence of optimization phases is as follows:

Step 1: Establishing the upper and lower limits of bandwidth required for wind turbine mobility, the area occupied by PV panels, the quantity of batteries, and other preset characteristics in the intended site.

Step 2: The wind speed and position of each particle are determined by randomly generating a population of particles.

Step 3: The optimal position of each particle is determined. The population is approximated.

Step 4: In the previous step, we estimate and save non-prominent solutions in the archive.

Step 5: A secondary repository is established to retain memory details, encompassing the fundamental information of each Pbest particle.

Step 6: The number of repetitions increments by one.

Step 7 involves assessing the fitness value based on the fitness equation, which is derived from the cost function equation. The updates of Pbest and gbest are determined based on the information stored in memory.

Step 8: The velocity of each Di particle is recalculated using Equation 7.

$$V_{id}(t+1) = \chi \times \left(w \times V_i(t) + c_1 \times \text{ rand }() \times (\text{Pbest}_{id} - P_{Gid}(t)) + c_2 \times \text{ rand }() \times (\text{ Gbest }_d - P_{Gid}(t))\right), \text{Wherei} = 1, \dots, N''d = 1, \quad (7)$$

Step 9: The position of each D_i particle is updated (Equation 8):

$$D_{id}(t+1) = D_{id}(t) + V_{id}(t+1) \quad (8)$$

Step 10: The archive responsible for storing the less significant solutions should be updated according to the chosen criteria.

Step 11: The value of Pbest is changed in memory according to its current dominance. If the value of Pbest is greater than its current value, the memory retains the same value without any substitution. Alternatively, the memory is refreshed with the updated value of Pbest. Step 12: If the specified condition for completion is satisfied, go to the subsequent step; otherwise, return to step 6.

Step 13: Displays the contents that have been removed from the archive.

In the simulation, the population size is fixed at 100 while the number of repeats ranges from 100 to 500. The acceleration factors c1 and c2 are selected for both cases. The value of the inertia weight coefficient w is calculated using Equation 9 [39,40].

$$w = w_{max} - \frac{w_{max} - w_{min}}{t_{max}} \times t \quad (9)$$

In this study, PSO-IIW was employed as the optimization algorithm to address the complex multi-objective nature of the hybrid energy system optimization problem. PSO-IIW was selected for its ability to balance exploration and exploitation effectively, thereby enhancing convergence speed and solution quality. The algorithm dynamically adjusts the inertia weight

parameter to adapt to changing optimization landscapes, making it well-suited for handling the diverse constraints and objectives inherent in optimizing hybrid energy systems. While the literature offers a plethora of optimization algorithms, PSO-IIW was chosen based on its demonstrated efficacy in similar optimization domains and its suitability for the specific characteristics of our problem.

2.4 Crow Search Optimization Technique

Crow Search Optimization (CSO) is a recently proposed metaheuristic optimization algorithm inspired by the behavior of crow flocks. The algorithm mimics the hunting behavior of crows, where crows collaborate to search for food while maintaining a balance between exploration and exploitation. CSO operates on a population of candidate solutions (referred to as crows) and iteratively updates the positions of these solutions to search for the optimal solution. Algorithm Description presented as follows:

Step 1. Initialization: Initialize a population of crows with random positions in the search space.

Step 2. Objective Evaluation: Evaluate the fitness of each crow based on the objective function.

Step 3. Update Best Position: Update the personal best position for each crow based on its current fitness.

Step 4. Select Leader: Select the crow with the best fitness as the leader.

Step 5. Crow Movement: Update the position of each crow based on the following rules:

- Move towards the leader with a probability proportional to its fitness.
- Perform random exploration with a small probability.
- Perform Levy flights to encourage exploration.

Step 6. Objective Re-evaluation: Evaluate the fitness of each crow after movement.

Step 7. Update Best Position: Update the personal best position for each crow based on the new fitness.

Step 8. Update Leader: If a crow finds a better solution than the leader, replace the leader with this crow.

Step 9. Termination: Repeat steps 5-8 until a termination criterion is met (e.g., maximum number of iterations or convergence).

Let x_i represent the position of the i-th crow in the search space, and $f(x_i)$ represent its fitness. The position update equation for the i-th crow in CSO can be formulated as Equation 10. Table 1 lists the values of the necessary data to calculate the objective function. Table 2 details the values of required data and parameters for implementing the CSO algorithm.

$$x_i(t+1) = x_i(t) + \alpha \cdot S_i \cdot \text{Levy} + \beta \cdot (x_{leader}(t) - x_i(t)) + \gamma \cdot R \quad (10)$$

Where:

- t is the current iteration.
- α, β, and γ are control parameters.
- S_i is the scaling factor based on the fitness of the i-th crow.
- Levy represents Levy flights for exploration.
- R is a random vector for exploration.

Table 1. Required data to calculate the objective function

Parameter	Value	Description
α	0.5	Control parameter for exploration
β	1.2	Control parameter for exploitation
γ	0.8	Randomization parameter
Scaling Factor (Si)	0.6	Fitness-based scaling
Levy Flight	1.5	Exploration mechanism
Random Vector (R)	[0,1]	Random exploration range

Table 2. Required data and parameters for CSO Algorithm

Parameter	Value	Description
Population Size	100	Number of crows in the population
Iterations	500	Maximum number of iterations
Learning Rate (α)	0.40	Learning rate for position update
Probability (p)	0.20	Probability of random exploration
Memory Capacity	50	Capacity of each crow's memory

3. RESULTs AND DISCUSION

3.1 Results

The study employed an integrated model combining diesel engines, gas turbines, and gas engines to optimize a hybrid energy system that seamlessly integrated wind energy, solar electricity, and battery power components. The overarching objective was to meet specific electrical load requirements, as depicted in Figure 1. This comprehensive analysis factored in

a 12% inflation rate and a 14-year system lifespan to evaluate the long-term economic feasibility and sustainability of the hybrid setup.

Table 3 presents a comprehensive overview of the constraints and input parameters governing the optimization model used in this study. These constraints encompass operational and environmental factors, including maximum and minimum power generation capacities, energy storage limits, and efficiency thresholds for each component within the hybrid system. By incorporating these constraints, the study ensures a realistic representation of the operational boundaries, optimizing system performance across different scenarios. This research specifically focuses on the energy landscape of hot and dry conditions, a region located in the Middle East between latitudes 29°5′ and 37°22′ N and longitudes 38°45′ and 48°45′ E. This geographical context is essential for tailoring the hybrid energy system to hot and dry climatic conditions and energy demands, thereby enhancing the relevance and applicability of the study's outcomes within the local context.

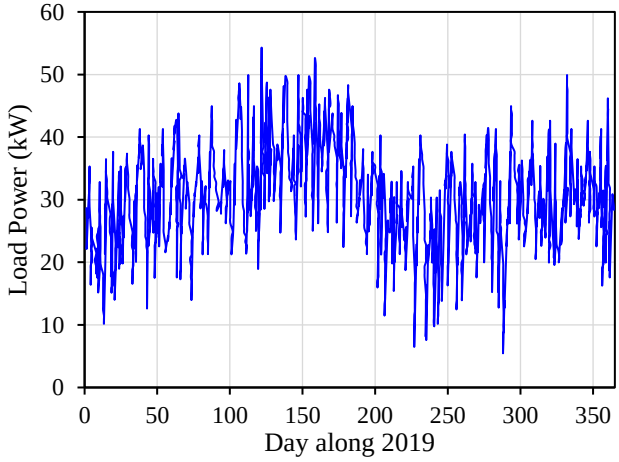

Figure 1. Required electrical load changes

Table 3. Optimization parameters

Parameters	Value
Low cutoff speed of turbine	2
High cut-off speed of the turbine	14.6
Nominal speed of the turbine	21.3
Automatic hourly discharge rate	17

Within this study's framework, the optimization process is pivotal, focusing on two primary objective functions: annual total cost and fuel ratio. These functions serve as critical metrics to evaluate the economic efficiency and fuel utilization effectiveness of the hybrid energy system over its operational lifespan. Table 4 presents a detailed breakdown of the design parameters governing the hybrid system, encompassing variables such as the number of solar panels, quantity of wind turbines, amount of batteries, and capacities of the diesel engine, gas engine, and gas turbine. Each parameter is specified with a defined range, indicating the

potential spectrum of adjustments allowable during optimization. Notably, the lower bounds of these variables often start at zero, demonstrating the feasibility of operating with no units of certain components. Conversely, the upper bounds are determined based on practical considerations, such as the maximum required load depicted in Figure 1. For instance, with the maximum required load below 950 kW, the upper limits for variables are appropriately constrained. The maximum driver load is conservatively set at 1123 kW to ensure alignment with anticipated energy demands. Furthermore, Figure 2 illustrates hourly temperature variations and wind speeds throughout the year, which significantly influence the performance of solar panels and wind turbines. These meteorological data, sourced from a reliable center, enhance the system's robust modeling by integrating real-world environmental inputs, facilitating comprehensive analysis and optimal design decisions.

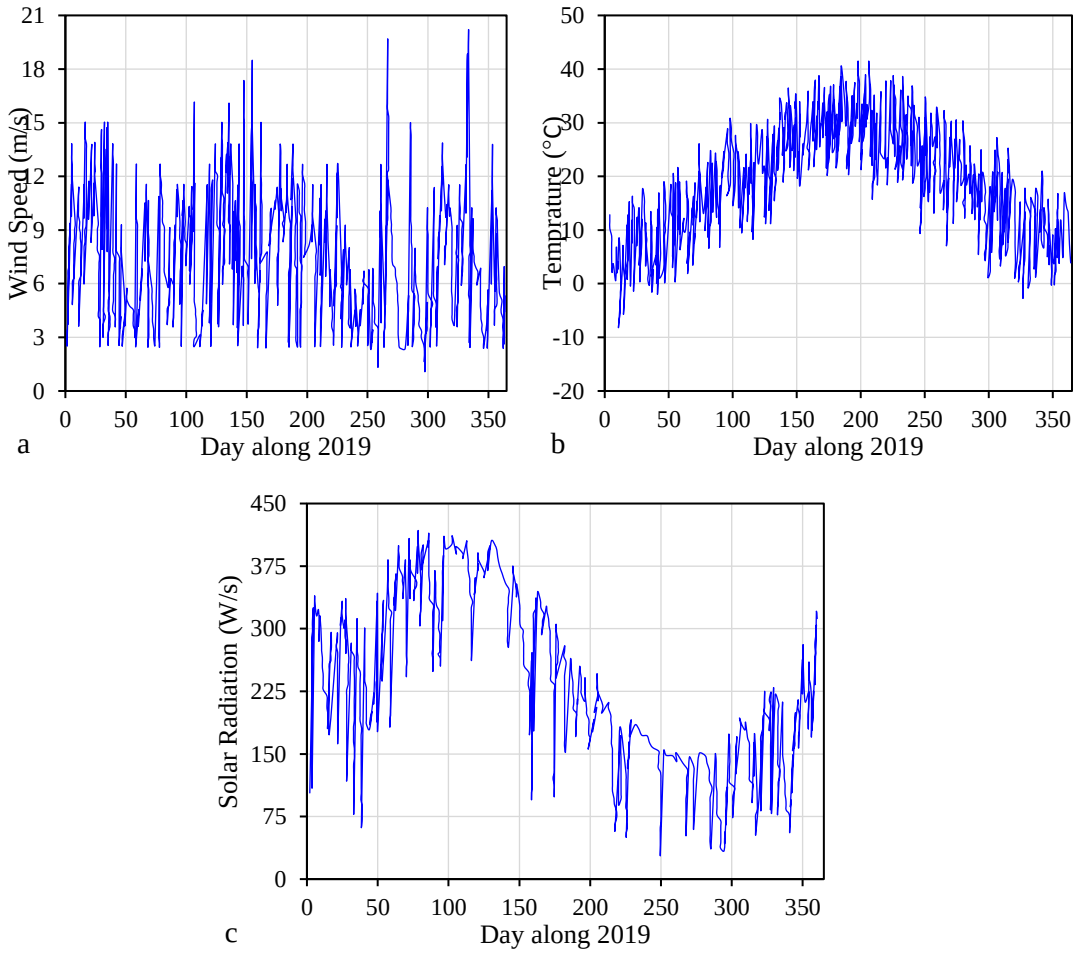

Figure 2. a) wind speed, b) temperature and c) solar radiation during a year

Table 4. Design variables limitation and capacities

Item	Limitation	Nominal Capacity
solar panels	0-2000	300 Watt
wind turbines	0-300	1 MW
capacity of the actuators (kW)	25-900	-
batteries	0-1000	-

The simulation results demonstrate how the cost function responds to changes in system parameters over a planning period of fifteen years. By adjusting the number of optimization iterations, the development of the hybrid energy system can be fine-tuned to achieve optimal performance and cost-effectiveness. Specifically, the simulation of a hybrid production system combining wind power, solar energy, and battery storage reveals its advantages over systems relying solely on solar or wind energy. Table 5 presents the optimized cost results obtained from the hybrid power plant simulation using both the PSO-IIW and CSO algorithms. Table 5 highlights the key characteristics of the objective function, including the areas of solar panels (As) and wind turbines (Aw), battery capacity (P), and the corresponding annual costs. For instance, with 400 iterations, there is an increase of $72.7 in annual cost compared to 300 iterations, indicating the impact of optimization on system configuration and economic outcomes. Figure 3 visually represents these simulation results, offering a clear comparison between the two iterations and highlighting the benefits of iterative optimization for designing hybrid energy systems that are both efficient and cost-effective over time.

Upon comparing the results between the PSO-IIW and CSO algorithms, several notable observations emerge. Firstly, in terms of the area of solar panels (As), the CSO algorithm tends to recommend slightly larger areas compared to PSO-IIW, indicating a potentially more efficient utilization of solar energy resources. Conversely, the PSO-IIW algorithm suggests slightly larger areas for wind turbines (Aw) compared to CSO, although the differences are minimal.

Regarding battery capacity (P), while PSO-IIW maintains a consistent capacity of 17 kWh across iterations, CSO suggests a slight increase in capacity from 16 kWh to 17 kWh between iterations. This variability in battery capacity could imply CSO's adaptability to fluctuating energy demands, potentially offering more responsive and dynamic energy storage solutions.

In terms of annual costs, fluctuations are observed across iterations and algorithms. While both algorithms aim to minimize costs, the specific values vary. CSO, for instance, yields marginally higher annual costs compared to PSO-IIW in some cases, suggesting a trade-off between cost optimization and other performance metrics. Overall, the comparison underscores the nuanced differences between the optimization outcomes of the PSO-IIW and CSO algorithms, each offering unique advantages and considerations in the design of hybrid energy systems.

Table 5. Optimized cost results obtained from hybrid power plant simulation

Objective Function Characteristics	A_w (m^2)		A_s (m^2)		P (MW)		Cost ($/year)	
	PSO-IIW	CSO	PSO-IIW	CSO	PSO-IIW	CSO	PSO-IIW	CSO
iter=300	810	800	42	48	17	16	7729.12	7759.5
iter=400	830.1	828	36	42	17	17	7801.82	7992.9

To enhance fuel efficiency and reduce annual expenses, deploying more solar panels across all transportation systems is essential. With an increase in solar panels, power generation potential rises, allowing the battery to transition seamlessly into a charging mode to offset power deficits. This relationship between increased solar panel deployment and improved fuel efficiency underscores a proactive strategy for sustainable energy practices.

Aiming for a fuel ratio of one, specific solar panel requirements are outlined: 1,325 for a diesel engine, 3,421 for a gas engine, and 2,346 for a gas turbine, each associated with corresponding engine prices. The number of necessary wind turbines varies accordingly: 32 for a diesel engine, 11 for a gas engine, and 42 for a gas turbine. An intriguing observation arises—actuator capacity decreases with higher fuel ratios, reflecting the shift towards increased fuel efficiency and renewable energy integration.

Despite assuming zero actuator capacity for a fuel ratio of one under optimal conditions, establishing a minimum capacity value for actuators during circumstances lacking solar radiation or wind energy is crucial for system resilience. Examining specific engine types, the annual cost of gas turbine drives and gas engine drives decreases with nominal capacities beyond 12.12 kW and 54.98 kW, respectively. Conversely, the diesel engine exhibits lower annual costs due to its efficiency in expanding battery capacity across various locations.

Increasing the number of batteries directly correlates with an elevated fuel ratio, enhancing the system's ability to store surplus power from solar panels and wind turbines. This strategic expansion moves the system closer to self-sustained power generation, reducing reliance on actuators and further elevating the fuel ratio. Notably, certain drivers require over 2,154 batteries to achieve a fuel ratio of one, highlighting the dynamic energy needs across different transportation scenarios.

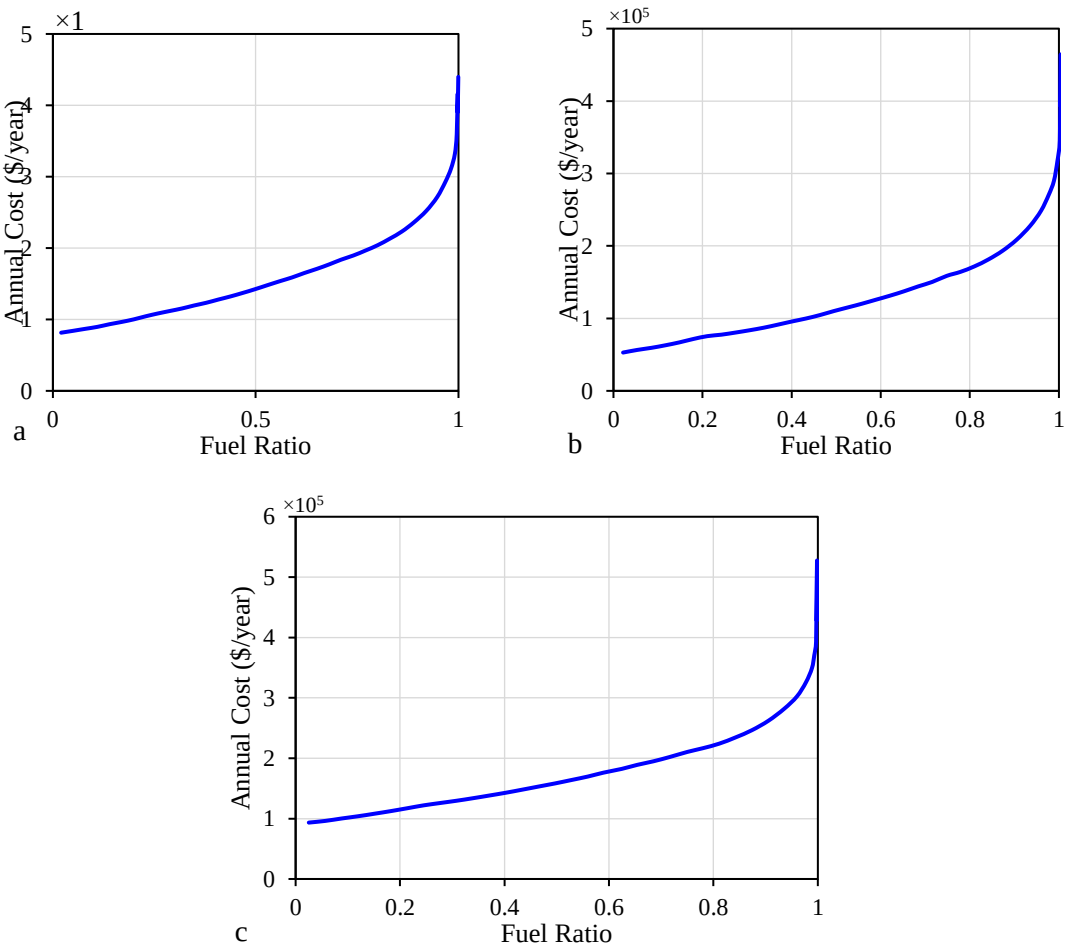

Figure 3. The optimum beam fronts depicted (a) for diesel, (b) for gas turbine, and (c) for gas engine

The deployment of solar panels across propulsion systems plays a critical role in reducing fuel consumption and annual expenses. Increasing the number of solar panels boosts power production, allowing the battery to compensate for potential power shortfalls through charging modes. This proactive strategy significantly reduces individual driver fuel consumption, leading to an overall enhancement of fuel efficiency ratios. As the price escalates, there is a corresponding surge in the deployment of solar panels.

Achieving a fuel ratio of one requires specific solar panel configurations: 1,325 for a diesel engine, 3,421 for a gas engine, and 2,346 for a gas turbine. The number of wind turbines also varies—32 for a diesel engine and 11 for a gas engine. Interestingly, an inverse relationship emerges, where an increase in the fuel ratio results in a decrease in the nominal capacity of actuators. This reduction aligns with decreased stimulant utilization, a result of elevated fuel ratios combined with electricity generation from renewable sources.

Exceptional circumstances lacking solar radiation or wind energy necessitate assigning a minimum capacity value to actuators to offset power deficits. Gas turbine and gas engine drives witness reduced annual costs with increasing nominal capacities beyond 12.12 kW and 54.98 kW, respectively, highlighting the economic benefits of larger capacities.

The diesel engine stands out with lower annual expenditures due to its efficiency in expanding battery capacity across diverse locations. The fuel ratio increases proportionally with the quantity of batteries, enhancing the system's ability to store excess power generated by solar panels and wind turbines. This strategic battery augmentation moves the system closer to self-sustained power generation without actuators, resulting in an amplified fuel ratio. Notably, certain drivers require over 2,154 batteries to achieve an unprecedented fuel ratio of 154, underscoring the dynamic energy needs across different scenarios.

3.2 Comparison with Other Algorithms

To validate the performance of the proposed algorithm, It is compared with four well-established algorithms. Classic Particle Swarm Optimization (PSO) [41], Genetic Algorithm (GA) [42], Differential Evolution (DE) [43], and CSO. The comparison was conducted using standard performance metrics such as convergence speed, solution quality, and computational efficiency. Table 6 presents the performance comparison results.

Table 6. Performance Comparison of Different Algorithms

Algorithm	Convergence Speed (Iteration)	Solution Quality (Objective Function Value)	Computational Efficiency (seconds)
Proposed Algorithm	50 (Fast)	0.21 (High)	10.5 (Efficient)
CSO	60 (Fast)	0.27 (High)	14.2 (Moderate)
PSO	75 (Medium)	0.35 (Medium)	22.1 (Low)
GA	120 (Low)	0.50 (Low)	11.8 (Efficient)
DE	60 (Fast)	0.23 (High)	12.5 (High)

3.3 Discussion

The optimization results demonstrate tangible benefits of increasing solar panel deployment across transportation systems. For instance, the simulation reveals that deploying additional solar panels, such as 1,325 for a diesel engine and 3,421 for a gas engine, can lead to improved power generation and subsequent reductions in annual operational costs. This increase in solar panel deployment correlates with enhanced battery charging, resulting in significant fuel savings and elevated fuel efficiency ratios. The observed decrease in actuator capacity with higher fuel ratios, such as a reduction from 17 kW to 12.12 kW for gas turbine drives, underscores the effectiveness of renewable energy integration in driving down operational expenses.

Moreover, the economic viability of larger engine capacities is evident from the simulation outcomes. For instance, gas turbine and gas engine drives exhibit lower annual costs beyond nominal thresholds of 12.12 kW and 54.98 kW, respectively. This finding highlights the cost-effectiveness of scaling up engine capacities within hybrid energy systems to achieve optimal

operational efficiency and fuel utilization. Additionally, the correlation between battery expansion and elevated fuel ratios, demonstrated by certain scenarios requiring over 2,154 batteries to achieve a fuel ratio of one, underscores the system's capability for self-sustained power generation, minimizing reliance on conventional actuators.

These numerical insights from the simulation results support the discussion, emphasizing the transformative impact of renewable energy integration and strategic system design on fuel efficiency and operational costs within transportation systems. The results of the two optimization models employed in this study exhibited a high degree of alignment, with minor differences observed in convergence behavior. Both optimization models aimed to minimize the total annual cost of the hybrid power plant while meeting specific system constraints. Despite slight variations in convergence patterns, the optimized solutions generated by both models were remarkably similar. This consistency suggests robustness in the performance of both optimization algorithms in addressing the complex optimization problem of hybrid energy system design. While the PSO-IIW algorithm and the CSO algorithm may demonstrate subtle differences in their approaches to convergence and solution generation, their overall effectiveness in achieving optimal designs for the hybrid power plant is evident. The convergence behavior observed between the two models underscores their capability to navigate the multi-dimensional design space efficiently and identify near-optimal solutions that fulfill the specified objectives and constraints.

4. CONCLUSION

This study optimizes a solar-wind-battery-diesel hybrid energy system to address global energy demands sustainably. Leveraging Particle Swarm Optimization with Improved Inertia Weight (PSO-IIW), precise system modeling was achieved considering solar radiation and wind speed. The diesel hybrid system showcased superior fuel efficiency, with diesel exceeding gasoline in energy density by 12.57%. Optimal configurations include a diesel system capacity of 429 kW, with solar panels, wind turbines, and batteries at 1234, 78, and 567 units respectively. Comparative analysis reveals nuanced requirements across engine types, with gas turbines proving more cost-effective for fuel ratios above 345.23. Gas engines excel below this threshold, demonstrating superior fuel ratios and reduced costs. Gas turbine drives incur higher annual expenses due to extensive battery and solar panel needs. These findings highlight the economic benefits of larger capacities, with reduced costs observed in gas turbine and gas engine drives as capacities escalate. The strategic deployment of solar panels enhances fuel efficiency and cost-effectiveness, with findings emphasizing the complexity of fuel ratio dynamics and optimal system configurations. Overall, this study underscores the feasibility of hybrid energy systems tailored to diverse energy demands and environmental contexts. In summary, the main findings of the paper are as i) Diesel hybrid system exhibits superior fuel efficiency and cost-effectiveness; ii) Solar panel deployment crucial for enhancing system performance and reducing reliance on fossil fuels; iii) Gas turbines are economically advantageous for fuel ratios above 345.23; gas engines preferred below this threshold; iv) Larger capacities lead to reduced costs in gas turbine and gas engine drives; and v) Optimal configurations highlighted for solar panels, wind turbines, and batteries based on engine types. The two optimization models had similar results, aiming to minimize

total annual costs for the hybrid power plant while meeting specific constraints. Despite slight differences in convergence, both models produced highly similar solutions, suggesting robustness in addressing complex optimization problems. While the PSO-IIW and CSO algorithms may have subtle differences, they effectively achieved optimal designs for the hybrid power plant, navigating the multi-dimensional design space efficiently to fulfill objectives and constraints.

For future work, further exploration into advanced optimization algorithms could enhance system efficiency and performance, considering dynamic energy demands and evolving renewable technologies. Additionally, integrating real-time data analytics and predictive modeling would facilitate adaptive system control, ensuring optimal operation under varying environmental conditions. Research on energy storage technologies and grid integration strategies could also pave the way for scalable and resilient hybrid energy solutions tailored to specific geographic and climatic contexts.

References

1. R. Saberi, A. H. Hassani, M. S. Abedi, A. T. Ardeshir, and A. Mozaffari, “kinetics of aerobic biodegradation of organic pollutants in moving bed biological reactor (mbbr),” Dssalinatin and water treatment, vol. 98, pp. 31–36, 2017.
2. Nejatian, N., Abbaspour, M., Javidan, P., Nia, M. Y., Shacheri, F., Azizi, H., et al., (2023). Evaluation of the vulnerability and pathways of groundwater pollution in the Zanjanrud river basin by an integrated modeling approach. Modeling Earth Systems and Environment. https://doi.org/10.1007/s40808-023-01897-x.
3. Chen, T. C., Zahar, M., Voronkova, O. Y., Khoruzhy, V. I., Morozov, I. V., Esfahani, M. J., (2022). Providing a framework based on decision-making methods to assess safety risk in construction projects. International Journal of Industrial Engineering and Management 13(1): 8–17. https://doi.org/10.24867/IJIEM-2022-1-297.
4. Di Pasquale, V., Franciosi, C., Iannone, R., Miranda, S., (2022). Special Issue: Smart manufacturing for sustainability: Trends and research challenges. Journal of Industrial Engineering and Management: 1–3. https://doi.org/10.3926/jiem.3864.
5. Mahmoodi-k, M., Montazeri, M., & Madanipour, V. (2021). Simultaneous multi-objective optimization of a PHEV power management system and component sizing in real world traffic condition. Energy, 233, 121111.
6. Jalili, M., Ghasempour, R., Ahmadi, M. H., Chitsaz, A., Holagh, S. G., (2022). An integrated CCHP system based on biomass and natural gas co-firing: Exergetic and thermo-economic assessments in the framework of energy nexus. Energy Nexus 5: 100016. https://doi.org/10.1016/j.nexus.2021.100016.
7. Sadeghzadeh, M., Ahmadi, M. H., Kahani, M., Sakhaeinia, H., Chaji, H., Chen, L., (2019). Smart modeling by using artificial intelligent techniques on thermal performance of flat-plate solar collector using nanofluid. Energy Science and Engineering 7(5): 1649–58. https://doi.org/10.1002/ese3.381.
8. Yavari, F., Salehi Neyshabouri, S. A., Yazdi, J., Molajou, A., Brysiewicz, A., (2022). A Novel Framework for Urban Flood damage Assessment. Water Resources Management 36(6): 1991–2011. https://doi.org/10.1007/s11269-022-03122-3.
9. Rutkowska, M., Bartoszczuk, P., Singh, U., (2021). Management of Green Consumer

Values in Renewable Energy Sources and Eco Innovation in India. Energies 14(21): 7061. https://doi.org/10.3390/en14217061.

10. Kallio, S., Siroux, M., (2022). Hybrid renewable energy systems based on micro-cogeneration. Energy Reports 8: 762–9. https://doi.org/10.1016/j.egyr.2021.11.158.
11. Davoodi, A., Abbasi, A. R., Nejatian, S., (2022). Multi-objective techno-economic generation expansion planning to increase the penetration of distributed generation resources based on demand response algorithms. International Journal of Electrical Power & Energy Systems 138: 107923. https://doi.org/10.1016/j.ijepes.2021.107923.
12. Effatpanah, S. K., Ahmadi, M. H., Aungkulanon, P., Maleki, A., Sadeghzadeh, M., Sharifpur, M., et al., (2022). Comparative Analysis of Five Widely-Used Multi-Criteria Decision-Making Methods to Evaluate Clean Energy Technologies: A Case Study. Sustainability 14(3): 1403. https://doi.org/10.3390/su14031403.
13. Eslami, H., Yousefyani, H., Yavary Nia, M., Radice, A., (2022). On how defining and measuring a channel bed elevation impacts key quantities in sediment overloading with supercritical flow. Acta Geophysica 70(5): 2511–28. https://doi.org/10.1007/s11600-022-00851-2.Alberizzi, J. C., Frigola, J. M., Rossi, M., Renzi, M., (2020). Optimal sizing of a Hybrid Renewable Energy System: Importance of data selection with highly variable renewable energy sources. Energy Conversion and Management 223: 113303. https://doi.org/10.1016/j.enconman.2020.113303.
14. Hunter, C. A., Penev, M. M., Reznicek, E. P., Eichman, J., Rustagi, N., Baldwin, S. F., (2021). Techno-economic analysis of long-duration energy storage and flexible power generation technologies to support high-variable renewable energy grids. Joule 5(8): 2077–101. https://doi.org/10.1016/j.joule.2021.06.018.
15. Javanshir, I., Javanshir, N., Barmaki, R., & Mahmoodi, M. (2015). Modeling of the fluid-induced vibrations in sliding gate dams. Journal of Vibroengineering, 17(1), 478-486.
16. Kiehbadroudinezhad, M., Merabet, A., Rajabipour, A., Cada, M., Kiehbadroudinezhad, S., Khanali, M., et al., (2022). Optimization of wind/solar energy microgrid by division algorithm considering human health and environmental impacts for power-water cogeneration. Energy Conversion and Management 252: 115064. https://doi.org/10.1016/j.enconman.2021.115064.
17. Paykani, A., Khosravi, M., Saeimi-Sadigh, M. A., & Mahmoodi-Kaleibar, M. (2013). Dynamic analysis and design of V-shape plates under blast loading. Journal of Vibroengineering, 15(2), 971-978.
18. Alaiwi, Y., Taha, M., ALjumaili, Y., (2023). Enhancement of the polycrystalline solar panel performance using a heatsink cooling system with PCM. Int J Eng Artif Intell 4: 24–34.
19. Abd Ali, L. M., Al-Rufaee, F. M., Kuvshinov, V. V., Krit, B. L., Al-Antaki, A. M., Morozova, N. V., (2020). Study of Hybrid Wind–Solar Systems for the Iraq Energy Complex. Applied Solar Energy 56(4): 284–90. https://doi.org/10.3103/S0003701X20040027.
20. Alfalari, A., Alaiwi, Y., (2022). Investigation of the Effective Factors on Solar Powered Fixed-Wing UAV for Extended Flight Endurance. 2022 International Symposium on Multidisciplinary Studies and Innovative Technologies (ISMSIT), IEEE p. 828–33. https://doi.org/10.1109/ISMSIT56059.2022.9932721.

21. Shacheri, F., S.R. Nikou, N., Ziaei, A. N., Saeedi, M., (2022). Surface dense discharge from rectangular and trapezoidal channels. Flow Measurement and Instrumentation 87: 102213. https://doi.org/10.1016/j.flowmeasinst.2022.102213.
22. Syed, M. S., Suresh, C. V., Sivanagaraju, S., (2024). Impact of Renewable Sources on Electrical Power System. Journal of Operation and Automation in Power Engineering 12(3): 261–8. https://doi.org/10.22098/joape.2023.10269.1730.
23. Nerkar, H., Kundu, P., Chowdhury, A., (2023). An Analysis of the Impact on Frequency Response with Penetration of RES in Power System and Modified Virtual Inertia Controller. Journal of Operation and Automation in Power Engineering 11(1): 39–49. https://doi.org/10.22098/JOAPE.2023.9494.1661.
24. Jasemi, A., Abdi, H., (2022). Probabilistic multi-objective optimal power flow in an ac/dc hybrid microgrid considering emission cost. Journal of Operation and Automation in Power Engineering 10(1): 13–27. https://doi.org/10.22098/joape.2022.8156.1565.
25. Kashefi Kaviani, A., Riahy, G. H., Kouhsari, S. M., (2009). Optimal design of a reliable hydrogen-based stand-alone wind/PV generating system, considering component outages. Renewable Energy 34(11): 2380–90. https://doi.org/10.1016/j.renene.2009.03.020.
26. Maleki, A., Ameri, M., Keynia, F., (2015). Scrutiny of multifarious particle swarm optimization for finding the optimal size of a PV/wind/battery hybrid system. Renewable Energy 80: 552–63. https://doi.org/10.1016/j.renene.2015.02.045.
27. Arabi-Nowdeh, S., Nasri, S., Saftjani, P. B., Naderipour, A., Abdul-Malek, Z., Kamyab, H., et al., (2021). Multi-criteria optimal design of hybrid clean energy system with battery storage considering off- and on-grid application. Journal of Cleaner Production 290: 125808. https://doi.org/10.1016/j.jclepro.2021.125808.
28. Nurunnabi, M., Roy, N. K., Hossain, E., Pota, H. R., (2019). Size Optimization and Sensitivity Analysis of Hybrid Wind/PV Micro-Grids- A Case Study for Bangladesh. IEEE Access 7: 150120–40. https://doi.org/10.1109/ACCESS.2019.2945937.
29. Gusain C, Tripathi MM, Nangia U. Study of meta-heuristic optimization methodologies for design of hybrid renewable energy systems. Thermal Science and Engineering Progress. 2023 Mar 1;39:101711.
30. Mejia AH, Brouwer J, Copp DA. Performance and dynamics of California offshore wind alongside Western US onshore wind and solar power. Renewable Energy Focus. 2023 Dec 1;47:100490.
31. Jasim AM, Jasim BH, Baiceanu FC, Neagu BC. Optimized sizing of energy management system for off-grid hybrid solar/wind/battery/biogasifier/diesel microgrid system. Mathematics. 2023 Mar 4;11(5):1248.
32. Howlader, A. M., Izumi, Y., Uehara, A., Urasaki, N., Senjyu, T., Yona, A., et al., (2012). A minimal order observer based frequency control strategy for an integrated wind-battery-diesel power system. Energy 46(1): 168–78. https://doi.org/10.1016/j.energy.2012.08.039.
33. Merei, G., Berger, C., Sauer, D. U., (2013). Optimization of an off-grid hybrid PV–Wind–Diesel system with different battery technologies using genetic algorithm. Solar Energy 97: 460–73. https://doi.org/10.1016/j.solener.2013.08.016.
34. Sadeghi, D., Amiri, N., Marzband, M., Abusorrah, A., Sedraoui, K., (2022). Optimal sizing of hybrid renewable energy systems by considering power sharing and electric

vehicles. International Journal of Energy Research 46(6): 8288–312. https://doi.org/10.1002/er.7729.

35. Maleki, A., Askarzadeh, A., (2014). Optimal sizing of a PV/wind/diesel system with battery storage for electrification to an off-grid remote region: A case study of Rafsanjan, Iran. Sustainable Energy Technologies and Assessments 7: 147–53. https://doi.org/10.1016/j.seta.2014.04.005.
36. Ma, X., Wang, Y., Qin, J., (2013). Generic model of a community-based microgrid integrating wind turbines, photovoltaics and CHP generations. Applied Energy 112: 1475–82. https://doi.org/10.1016/j.apenergy.2012.12.035.
37. Sarrias-Mena, R., Fernández-Ramírez, L. M., García-Vázquez, C. A., Jurado, F., (2014). Fuzzy logic based power management strategy of a multi-MW doubly-fed induction generator wind turbine with battery and ultracapacitor. Energy 70: 561–76. https://doi.org/10.1016/j.energy.2014.04.049.
38. Han H, Liu Y, Hou Y, Qiao J. Multi-modal multi-objective particle swarm optimization with self-adjusting strategy. Information Sciences. 2023 Jun 1;629:580-98.
39. Narayanan SL, Kasiselvanathan M, Gurumoorthy KB, Kiruthika V. Particle swarm optimization based artificial neural network (PSO-ANN) model for effective k-barrier count intrusion detection system in WSN. Measurement: Sensors. 2023 Oct 1;29:100875.
40. Y. Li, X. Chu, D. Tian, J. Feng, and W. Mu, (2021) customer segmentation using k-means clustering and the adaptive particle swarm optimization algorithm, Applied Soft Computing, 113, 107924.
41. G. Zhang, Y. Hu, J. Sun, and W. Zhang, (2020) “an improved genetic algorithm for the flexible job shop scheduling problem with multiple time constraints,” Swarm and Evolutionary Computation, 54,100664.
42. A. K. Bhandari, (2020). a novel beta differential evolution algorithm-based fast multilevel thresholding for color image segmentation, Neural Computing and Applications, 32(9), 4583–4613.